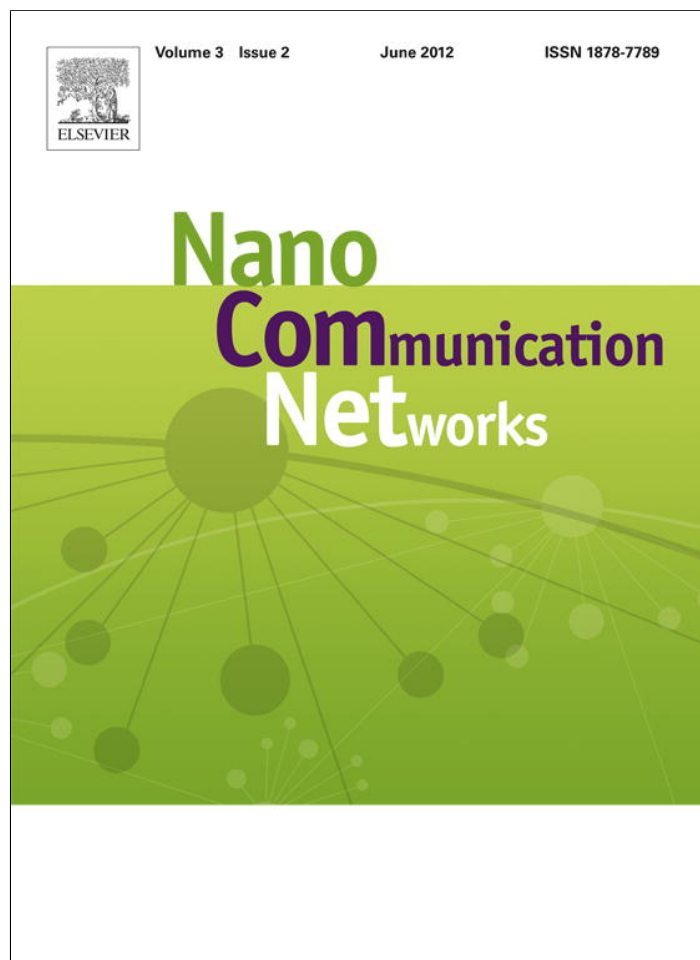


Provided for non-commercial research and education use.
Not for reproduction, distribution or commercial use.



This article appeared in a journal published by Elsevier. The attached copy is furnished to the author for internal non-commercial research and education use, including for instruction at the authors institution and sharing with colleagues.

Other uses, including reproduction and distribution, or selling or licensing copies, or posting to personal, institutional or third party websites are prohibited.

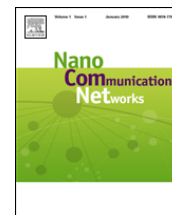
In most cases authors are permitted to post their version of the article (e.g. in Word or Tex form) to their personal website or institutional repository. Authors requiring further information regarding Elsevier's archiving and manuscript policies are encouraged to visit:

<http://www.elsevier.com/copyright>



Contents lists available at SciVerse ScienceDirect

Nano Communication Networks

journal homepage: www.elsevier.com/locate/nanocomnet

Molecular coordination of hierarchical self-assembly

Bruce J. MacLennan*

Department of Electrical Engineering and Computer Science, University of Tennessee, Knoxville, TN 37996-3450, USA

ARTICLE INFO

Article history:

Received 14 November 2010

Received in revised form 24 October 2011

Accepted 18 January 2012

Available online 8 February 2012

Keywords:

Embodied computation

Molecular communication

Morphogenesis

Nano communication

Self-assembly

Self-organization

ABSTRACT

A serious challenge to nanotechnology is the problem of assembling complex physical systems that are structured from the nanoscale up through the macroscale, but embryological morphogenesis provides a good model of how it can be accomplished. We review the fundamental processes in embryological development and argue that these processes, or approximations to them, will be feasible in artificial morphogenetic systems. Nevertheless, there are differences between natural and artificial systems, which future research must address. We explain the approach we are taking toward morphogenetic programming, present a notation for describing morphogenetic programs, and present two examples: the routing of neuron-like connections and the assembly of a segmented body frame with segmented legs by a clock-and-wavefront mechanism. Although much research remains to be done, we show how to implement the fundamental processes of morphogenesis and thereby coordinate very large numbers of agents to self-assemble into multiscale complex hierarchical systems.

© 2012 Elsevier Ltd. All rights reserved.

1. Introduction

1.1. Hierarchical self-assembly

There has been rapid progress in nanotechnology, but much of it is still at the level of producing novel materials, which must be assembled into macroscopic systems by conventional manufacturing techniques. The value of this approach cannot be denied, because it permits new materials to be integrated into a well-developed manufacturing technology. Complex natural systems are quite different, however, for they grow and develop through self-organization, at many scales from the nanoscale (nanometers) up through the macroscale (meters). Even conventional computer systems exhibit many hierarchical levels, from submicron features, up through devices and circuits, to millimeter-scale cores and chips, to boards and manufactured products. How can we produce artificial systems exhibiting complex structure at many size scales, from nanometers to meters?

1.2. Embryological morphogenesis as a model

Embryological development provides an inspiring example of how an extremely complex, hierarchically structured system can organize itself from the nanoscale up to the macroscale. From the nanoscale structures within cells, up through the assembly of cells and other materials into tissues, and tissues into organs, and organs into a living organism. Especially inspiring is the self-organization of the nervous system, which assembles some dozens of neurons into cortical minicolumns, dozens of minicolumns into macrocolumns, tens of thousands of macrocolumns into functional regions (such as the 52 Brodmann areas), and connects these regions into an integrated brain with perhaps 100 billion neurons and tens of thousands of connections per neuron.

Although there is much that we do not know about embryological development, it is clear that it is a process that is primarily self-organized but also conditioned by interaction with the environment [13]. Mechanochemical processes are the principle agents of *morphogenesis* (creation of three-dimensional physical form), for molecules mediate both communication and the bonds that transmit mechanical force. Therefore, aside from its practical

* Tel.: +1 865 974 5067.

E-mail address: macleannan@eecs.utk.edu.

applications in nanotechnology, morphogenesis can teach us how molecular communication and control can coordinate nanoscale assembly.

1.3. Self-assembly of robots

While there will be many applications of multiscale hierarchical self-organization in nanotechnology, one of the most compelling is the assembly of future robots and their components. Advanced robotic systems will require sensors, effectors, and control systems with a complexity approaching or even exceeding corresponding natural systems.

For example, we would like to have an artificial retina with capabilities comparable to the human retina, which comprises some 100 million sensors and intraretinal neural processing that compresses the data into about a million optic nerve fibers. To construct an artificial retina of comparable complexity, we will need to assemble hundreds of millions of components into a functional organization, and self-organization seems the most promising approach.

Artificial robot skin is another good candidate for artificial morphogenesis. Our ability to grasp objects securely but delicately, and to manipulate them flexibly, depends on detailed haptic and cutaneous input from millions of sensors in our skin, underlying flesh, joints, etc. How can these sensors be incorporated into a flexible but tough artificial skin and be appropriately connected to the robot's central control and coordination system? Artificial morphogenesis is a promising possibility.

Likewise, effectors capable of delicate, highly coordinated movement may require artificial muscles with a complex micro- or nanostructure. In humans and other vertebrates, millions of neurons control individual muscle fibers in order to achieve fluent motion.

Recent decades have demonstrated the value of neural networks for implementing adaptive cognitive and control systems. But brain-scale artificial neural networks will require new approaches to creating artificial neurons and assembling them into functional circuits. The best example of how to do this is the embryological development of the vertebrate brain. Likewise, the “nerves” of such robots will have to be wired in a self-directing fashion. In addition to the difficulty of routing them, their inputs and outputs will be into dense sensor, actuator, and neural arrays comprising large numbers of microscopic elements.

The foregoing are some of the reasons that we have been investigating *artificial morphogenesis*, which is the application of processes inspired by embryological development to the self-assembly of hierarchically structured three-dimensional forms [21,23–26].

2. Fundamental morphogenetic processes

What are the fundamental mechanisms of embryological morphogenesis? Edelman has categorized the primary processes of morphogenesis into *driving forces* and *regulatory processes* [13, p. 17] (see Table 1). The three driving forces are cell division, cell death, and cell movement, and

Table 1
Fundamental morphogenetic processes [13].

Driving forces	Cell division Cell death Cell movement
Regulatory processes	Cell adhesion Cell differentiation

Table 2
Specific morphogenetic processes [30].

Cell autonomous mechanisms	Division of heterogeneous egg Asymmetric mitosis Internal mitotic dynamics
Inductive mechanisms	Hierarchical Emergent
Morphogenetic mechanisms	Directed mitosis Differential growth Apoptosis Migration Chemotaxis Haptotaxis Chemokinesis Differential adhesion Contraction Matrix deposition and loss
Inductive–morphogenetic interactions	Morphostatic Morphodynamic

the two regulatory processes are cell adhesion and cell differentiation. Some of these processes have obvious analogs in artificial systems, but others do not, an issue we address later (Section 3.2).

More specifically, biologists have identified a dozen or so processes that seem to be sufficient for natural morphogenesis, summarized into a convenient taxonomy by Salazar-Ciudad et al. [30] (see Table 2). First, they distinguish (1) *cell autonomous* mechanisms, in which cells do not interact, (2) *inductive* mechanisms, in which cells signal each other, resulting in a change of cell state, and (3) *morphogenetic* mechanisms (in the narrow sense), in which cells interact, resulting in pattern changes but not state changes.

There are three cell autonomous mechanisms: *division of a heterogeneous egg*, in which a heterogeneous distribution of proteins and other materials in the egg leads to a heterogeneous distribution in the daughter cells, *asymmetric mitosis*, in which gene products are differentially transported to the daughters during cell division, and *internal temporal dynamics coupled to mitosis*, in which cyclic expression of genes is uncoupled with the cell cycle, so that daughter cells acquire different states. Since artificial morphogenesis is unlikely to use self-reproduction as a means of tissue growth (see Section 3.2), we expect cell autonomous mechanisms to take a smaller role in artificial morphogenesis than in its natural inspiration; their role in complex pattern creation is in any case limited [30]. Rather, in artificial morphogenesis newly arriving agents will have their states determined by agents already present, primarily by inductive mechanisms, to which we now turn.

Inductive mechanisms may be classified as *hierarchical* or *emergent*, both of which involve cell signaling

(1) by means of secretion of diffusible chemicals, (2) by membrane-bound chemicals, or (3) by direct signaling through cell-to-cell junctions. Hierarchical induction refers to mechanisms by which one group of cells influences another, but in which any backward signaling does not affect the first group's signaling. This is not the case for emergent (or self-organizing) induction, in which there are reciprocal effects between signaling regions. Examples include reaction–diffusion processes, which are basic to embryological pattern formation [27,33]. In general, emergent mechanisms seem more capable of producing a variety of complex patterns than hierarchical ones [30].

This is also the case for morphogenetic mechanisms (in the narrow sense of processes that rearrange cells without altering their states), which depend on the mechanical properties of cells and the extracellular matrices, including their viscosity, elasticity, and cohesiveness [30]. One of these morphogenetic mechanisms is *directed mitosis*, which causes daughter cells to be located at specific positions relative to an oriented mother cell; although artificial morphogenesis might not use mitosis, a similar effect can be achieved by having newly arriving agents assume an orientation with respect to existing agents. A mechanism more appropriate to artificial morphogenesis is *differential growth*, in which regions growing at different rates can affect the developing form. *Apoptosis* (programmed cell death) can lead to a change of form through the consequent rearrangement of the regions surrounding a cavity resulting from cell death. Although artificial agents do not literally die, the effect of apoptosis can be achieved by having agents leave the system or by having them disassemble themselves (see also Section 3.2).

Migration is a fundamental morphogenetic mechanism, in artificial systems as well as natural. Movement may be guided by a chemical gradient (*chemotaxis*) or by an adhesive gradient in an insoluble substrate (*haptotaxis*), and non-directed movement may be speeded or slowed by an ambient chemical signal (*chemokinesis*). This is the heart of molecular communication in morphogenesis, and it is here where we see most clearly the role of molecular coordination in self-assembly. However, full exploitation of these processes will require the development of artificial agents able to respond to molecular signals and to control their molecular interaction with other active agents and with inactive structures.

Differential adhesion is a morphogenetic mechanism by which cells can sort themselves into distinct populations [5,18]; combined with cell anisotropy and non-uniformly distributed adhesive molecules, differential adhesion can lead to the formation of lumens (cavities), invaginations, evaginations, and other functional forms [15, ch. 4]. Differential adhesion is also fundamental to epithelial–mesenchymal transformations, in which epithelia “dissolve” into mesenchyme or mesenchyme condenses into epithelium [13, pp. 67–71]. We expect differential adhesion to play an important role in artificial morphogenesis, since there are variety of ways to control adhesion between artificial agents (Section 3.2).

Contraction is a morphogenetic process resulting from individual cell contraction, which can change the shape of tissues, either by direct cell-to-cell connection in

epithelium or by mechanical transmission through an extracellular matrix in mesenchyme. Therefore it will be useful if artificial morphogenetic agents also have some ability to change their shape.

The last class of morphogenetic processes affects the viscoelastic extracellular matrix, leading to a change of tissue shape. For example, cells may add to or degrade the matrix material, or through hydration cause existing matrix material to swell. We expect that artificial morphogenesis will also make use of *matrix deposition and loss*, perhaps in preference to mitosis and apoptosis, by having artificial agents secrete, absorb, or otherwise manipulate inert materials and inactive components.

Finally, Salazar-Ciudad et al. [30] observe that inductive and morphogenetic mechanisms can interact in two fundamentally different ways. Simplest is *morphostatic* interaction, in which inductive mechanisms establish “genetic territories” (or “morphogenetic fields”) on which, afterwards, morphogenetic mechanisms operate. That is, induction establishes a spatial pattern of cell states, which then govern the morphogenetic reshaping of three-dimensional form. In contrast, induction and morphogenesis are simultaneous in *morphodynamic* interaction, which is therefore much more complicated to understand, but also more capable of producing complex patterns and forms. The challenge for artificial morphogenesis is to understand both morphostatic and morphodynamic interactions in order to self-assemble complex, functional hierarchical structures.

3. Artificial morphogenesis

3.1. Morphogenesis as embodied computation

Natural morphogenesis is an example of *embodied computation*, in which physical processes are directly exploited for computation and control [21,23–26,19]. The fundamental morphogenetic processes described in Section 2 provide many examples of how physical properties and processes are recruited to create complex, hierarchical structures. To apply embodied computation in artificial morphogenesis, however, it is not necessary to copy the exact physical mechanisms of natural morphogenesis. Rather, we seek to express the natural processes in abstract mathematical form, and then develop alternate physical systems that conform to these mathematical descriptions. For example, a given abstract reaction–diffusion system can be realized in various media, so long as the required parametric relations are preserved. The mathematical descriptions are in effect programs that can be realized in a variety of physical systems; what makes embodied computation different from ordinary computation is that we adhere closer to the physics, which facilitates applying computational ideas at the nanoscale [20].

Artificial morphogenesis has some characteristics in common with *amorphous computing* [1], but as the morphogenetic process proceeds, the medium becomes less and less amorphous: earlier forms structure and constrain the computation and control processes that create later forms. Also related to our project are ongoing efforts in modeling natural morphogenesis, which are relevant to

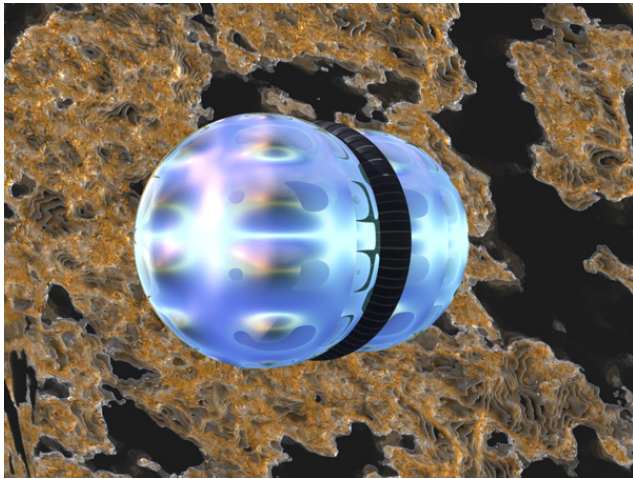


Fig. 1. Artistic depiction of microrobot. Such a microrobot might have molecular sensors and actuators to allow temporary or permanent attachment to other microrobots or to inactive components. At least limited ability to change shape would be useful for artificial morphogenesis.

our research, although their goal is different from our intended application area, namely nanotechnology. There is also related research applying morphogenetic ideas to reconfigurable robotics [16,28,29], but we do not believe that the techniques hitherto developed will scale up to the very large numbers of agents that is our goal (hundreds of thousands to hundreds of millions).

3.2. Natural vs. artificial morphogenesis

It is certainly conceivable that artificial morphogenesis might be accomplished by genetically engineering microorganisms or other cells to have the required behavior, thus closely imitating natural morphogenesis. However, we are also concerned with nanoscale assembly by microscopic artificial agents (e.g., microrobots, Fig. 1), and so we cannot assume all of the capabilities of living cells.

In particular, for the foreseeable future, self-reproduction will be beyond our capabilities. Since cell division leading to tissue growth is a fundamental *driving force* in natural morphogenesis (Section 2), artificial morphogenesis will have to accomplish tissue growth by other means. One obvious approach is to attract agents to regions of tissue growth from an external source (Fig. 2). The problem with this is that there must be a passage from outside the tissue and giving access to growth areas, which is not the case for cell division, which can occur in the interior of a growing tissue. An alternative approach is to have active agents transport inactive materials or structures and to deposit them at growth sites, but this also requires access to the growth sites. The path to the growth area does not have to be empty; for example it could be a fluid or visco-elastic medium that the agents can penetrate.

Whatever process is used in place of cell-proliferation, it should also serve as a substitute for directed mitosis, in which daughter cells have a specific orientation with respect to the mother cell's orientation. This may be accomplished by having newly arriving artificial agents align themselves with already assembled agents, or by having them deposit inactive structures in the correct orientation.

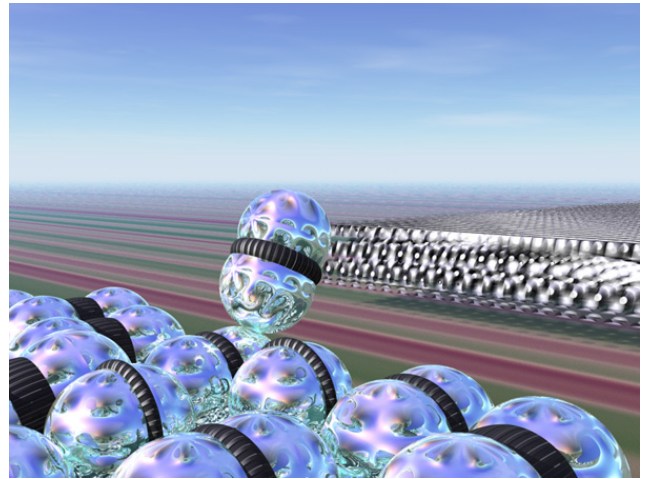


Fig. 2. Artistic depiction of microrobots self-assembling to form artificial tissues. Microrobots might use molecular or electrostatic means of adhering to each other or to other, inactive structures or components.

So the biological processes have to be accomplished by different means.

Programmed cell death (apoptosis) is also another one of the driving forces in embryological morphogenesis; by forming cavities in tissues it reshapes and sculpts them. It is certainly simple enough to have an artificial agent turn itself off; what is not so easy is to have its material reabsorbed, creating a cavity where it was. Depending on its material structure, an agent may be able to trigger its own disassembly, with subsequent physical processes transporting the waste materials away.

The third driving force in natural morphogenesis is cell migration, which is often implemented by changes in adhesion (to other cells and to the extracellular matrix) and in cell shape (e.g., extending lamellipodia) [13, ch. 7]. Cells control adhesion by means of a number of *cell adhesion molecules* (CAMs) and *substrate adhesion molecules* (SAMs), which are distributed on the cell membrane by a controlled but stochastic process. It seems unlikely that nonbiological agents will be able to make use of the same variety of CAMs and SAMs, and so we may have to adjust morphogenetic processes to get by with fewer of them. Goldstein et al. [16] have suggested electrostatic adhesion as an alternative to molecular adhesion, but it is unclear whether it will have the specificity required for artificial morphogenesis.

Cell adhesion is also one of the two morphogenetic *regulatory mechanisms* identified by Edelman (Section 2). In addition to its function in cell migration and in implementing rigid and elastic tissues, cell adhesion produces signals regulating cell differentiation and epithelial–mesenchymal transformations. In these cases, artificial morphogenesis may be able to make use of a variety of (nonadhesive) signals in combination with a small number of generic adhesion mechanisms.

The other morphogenetic regulatory mechanism is cell differentiation, which is both the means and end of embryological development. Since an embryo's cells are genetically identical, they differentiate by modulating their genetic regulatory mechanisms, thereby changing their properties and behavior. These protein and genetic regulatory networks have many of the abstract characteristics of electrical circuits and can be understood in

analogous abstract terms [7,8]. Similarly, artificial morphogenetic agents can change internal control states in order to modify their behavior. However, there are other approaches applicable to artificial morphogenesis, since in the absence of self-reproduction there is no requirement that all agents be identical. Since agents are being supplied from an external source, they may be provided in several different varieties. This approach has its own complications, since agents of different types have to be able to find their ways to the places where they belong, rather than differentiating *in situ*. Another alternative to differentiation is to have agents transport various inactive components to their destinations, but this does not solve the problem of getting to the destination. Therefore, artificial morphogenesis can use processes inspired by embryological development, but some adjustments will be required.

As explained in Section 1.3, future robotic systems will require artificial morphogenesis for their assembly. In particular, we expect that intermediate and long distance connections will be required, for example, to implement the robotic “nervous system”. During embryological development, neurons send out long projections (*neurites*), which find their way to their destinations, primarily by following chemical signposts. It seems unlikely that foreseeable microrobots will be able to change their shape and grow to this extent, so artificial morphogenesis may have to find alternative approaches to create long distance connections. For example, a microrobot (analogous to a neural *growth cone*) can follow the signposts, creating a path from the origin to the destination by depositing some substance in its wake. (See Section 5, below, for a simulation of an artificial morphogenetic program for generating such connections.)

4. Morphogenetic programming

4.1. Continuous models

One goal of our research has been to develop a methodology for *morphogenetic programming*, that is, for describing morphogenetic processes in a way that helps to understand their abstract structures independently of specific material realization, thus facilitating their use in artificial morphogenesis. In particular, we seek to understand their communication and control structures, and so we have been designing a sort of “morphogenetic programming language” [21,23–26] (see Section 5 for examples).

Biologists use a variety of tools to describe morphogenesis, including agent-based models [6], *influence diagrams* [32], and mathematical equations. In particular, although cells are discrete, biologists have often found it worthwhile to treat tissues as continua, and so partial differential equations (PDEs) and continuum mechanics have proved to be useful tools for analyzing embryological morphogenesis [27,5,15,31]. In our work too we are focusing on continuous mathematics, in particular to ensure that our morphogenetic processes scale up to very large numbers of agents (hundreds of thousands, millions, or even billions). Although we do not have the technology to do this yet, we are confident that it will come, and so we want to ensure that our techniques will scale. Going to the continuum limit

(an infinite number of infinitesimal agents) is one way to do this, a conclusion supported by the use of PDEs in embryology.

Nevertheless, cells are active agents, and so biologists have also found it worthwhile to adopt an agent-oriented perspective [6]. In our approach, we integrate an agent-oriented perspective with continuous mathematics by using a *material* or *Lagrangian* reference frame, as is common in continuum mechanics [21,23,24,26]. In this way, we can understand morphogenetic processes in terms of infinitesimal points moving through space and transporting their intrinsic properties (corresponding to cell state, for example). In some cases it is more convenient to take an external perspective in a fixed Eulerian reference frame, but it is mathematically easy to convert between the two reference frames.

In natural morphogenesis there are clearly cases where the continuum approximation is inappropriate, such as when the cell number is very small in the early stages of development. Although, in the absence of self-reproduction, the situation is different in artificial morphogenesis, there are cases where the density of agents in a particular state or of inactive components is so small that small-sample effects are relevant, for example, for symmetry breaking. Therefore, artificial morphogenesis cannot ignore ranges of phenomena where the continuous approximation begins to break down [21,26].

The goals of artificial morphogenesis have led us to a somewhat different approach to modeling morphogenetic processes than those used in a biological context. For example, COMPUCELL3D is an important tool for modeling biological morphogenesis [9]. However, it models phenomena at a much lower level than we do, for it uses a cellular Potts model on a mesh smaller than a single cell to model changes in cell shape. In contrast, the points of our continua represent an indeterminate number of agents with single-valued mathematical variables (even if, in some cases, they are random variables). For example, a single material point in a tissue might represent a set of agents with a particular orientation moving with a particular velocity.

By using PDEs and continuum mechanics, we work at a level that permits complementary interpretations of tissues as either continua or large discrete ensembles. Such complementary interpretations are common in physics and biophysics: PDEs are often used to describe fluids composed of discrete particles, atoms, molecules, or cells, and conversely PDEs are computationally simulated on discrete meshes. Additional details of our approach can be found in previous publications [21,23,24,26].

4.2. Change equations

The foregoing discussion advocates complementarity in the spatial domain, but we have also found it valuable to maintain complementary continuous and discrete interpretations in the time domain. Biologists often use differential equations to describe morphogenetic phenomena, even though many of the underlying cellular processes are discrete events; this is justified in part by the fact that they are stochastic and in part by the fact that the

equations are applied to populations of cells. On the other hand, simulations of these processes on digital computers proceed by discrete time steps. For these reasons, in artificial morphogenesis we make use of a notation that has consistent complementary interpretations as either a differential equation or a difference equation. Specifically, the *change equation*

$$\mathfrak{D}X = F(X, Y, \dots)$$

can be interpreted as a differential equation $\partial X/\partial t = F(X, Y, \dots)$ or as a finite difference equation $\Delta X/\Delta t = F(X, Y, \dots)$, where $\Delta X(t) = X(t + \Delta t) - X(t)$ and the time increment Δt is implicit in the notation. The formal rules of manipulation for the \mathfrak{D} operator respect its complementary interpretations.

4.3. Descriptive hierarchy

The goal of artificial morphogenesis is to apply in nanotechnology the processes that occur in natural morphogenesis or analogous processes that are inspired by them. Therefore, our goal is to understand the essences of the natural processes, to separate them from their specific physical realizations, so that they can be realized in different physical systems for technological purposes. If a description of a process is too specific, it may have a limited range of potential realizations, and thus be less applicable and useful in general. On the other hand, if a description is not specific enough, then it may leave essential component processes unexplained, which may turn out to be difficult or impossible to implement. (The same problem can arise in rigorously applied top-down programming.)

For example, as previously discussed, tissue growth in embryos is a result of cell division, but for a morphogenetic process to function, it may be sufficient that the tissue grow, regardless of how this is accomplished. For example, in an embryo the increasing density of cells resulting from cell division increases the tissue's dimensions. However, in an artificial system the dimensions of a tissue might increase through agent motion, and the decreasing agent density could attract new agents from an external supply to compensate. The essence of the process, its generic description, is tissue growth with a constant density; it can be realized in the preceding two ways and others. (See Sections 5 and 6 for examples.)

Our morphogenetic programming notation has a construct called a *substance* that has similarities to a *class* in object-oriented programming (Section 5). As in object-oriented programs, a subclass can further specify the behavior of a class, resulting in a class hierarchy, so in morphogenetic programming substances are defined in hierarchies of more or less specificity [21,23,24,26].

4.4. Conditional notation

Thresholds are common in morphogenesis and in many embodied computational processes; often a process takes place only if some quantity is above or below a threshold, which may be fixed or depend on other quantities. Thresholds are expressed conveniently by use of the *Heaviside* or *unit step function*:

$$u(x) = \begin{cases} 1, & \text{if } x > 0 \\ 0, & \text{otherwise.} \end{cases}$$

For an example, consider the change equation:

$$\mathfrak{D}y = u(x - \vartheta)\kappa(1 - y).$$

So long as x is above the threshold ϑ , y will increase with rate constant κ until it saturates at $y = 1$. Of course, in the context of real, physical processes, a discontinuous step function is only an approximation to reality, and soft thresholds are more realistic. Nevertheless, we may use hard thresholds as a first approximation.¹

Since this usage of the Heaviside function is so common in artificial morphogenesis, we introduce a special “conditional notation” for it, $[x > \vartheta] = u(x - \vartheta)$, so the preceding equation can be written as

$$\mathfrak{D}y = [x > \vartheta]\kappa(1 - y).$$

This makes clear the conditions under which y increases. Obvious extensions of the notation are permitted:

$$[x < y] = u(y - x),$$

$$[x > y \wedge a < b] = u(x - y)u(b - a),$$

$$[x \geq y \vee a \leq b] = 1 - u(y - x)u(a - b),$$

$$[x > y > z] = u(x - y)u(y - z),$$

etc.

In the physical context of embodied computation, there is no practical difference between strict and non-strict inequalities (e.g., between $x > y$ and $x \geq y$).

4.5. Partial equations

Morphogenetic and other cellular regulatory processes often have a “bow tie” organization, in which many processes contribute to the determination of a quantity, which in turn regulates many other processes. As a consequence, the change equation for such a quantity may have many terms on its right-hand side, and for convenience we allow such equations to be broken into multiple *partial change equations*. For example,

$$\mathfrak{D}R = [B < \vartheta_B]\kappa_R S(1 - R) + D_R \nabla^2 R - R/\tau_R$$

can be written as the two partial equations:

$$\mathfrak{D}R + = [B < \vartheta_B]\kappa_R S(1 - R),$$

$$\mathfrak{D}R + = D_R \nabla^2 R - R/\tau_R.$$

The partial equations do not have to be consecutive, as here, but may be interspersed with other partial or complete change equations. This notation also facilitates incremental development of morphogenetic processes. It was first used for morphogenetic programming by Kurt Fleischer [14, p. 20], but descends ultimately from the programming language ALGOL 68 [34].

5. Example: path routing

To illustrate one mechanism by which long range connections might be established, as for an artificial neural cortex [22], we present a path-routing process inspired by neuron growth. The goal is to make paths

¹ Fleischer [14, pp. 20–21] defines a notation for soft conditions.

through a three-dimensional medium from specific origins to corresponding destinations without colliding with (or coming too close to) existing paths.

The destination secretes an *attractant* A , which diffuses through the medium and degrades (or leaves the system) at certain rates. Existing paths clamp the attractant concentration to 0. A body of agents (which, by analogy with neurogenesis, we call a *growth cone*) follows the gradient of the attractant at a constant velocity, which leads it to the destination while avoiding collisions with existing paths.

As the growth cone moves through the medium, it creates the path in its wake. This is a case where a process is described generically to permit multiple realizations (as discussed previously, Section 4.3). In biological neurogenesis, the growth cone is the growing tip of a neuron's axon, and the path is created by cell growth and shape change. However, such drastic change of shape and size may be infeasible for artificial agents, such a microrobots. Instead, a fixed body of agents constituting the growth cone might create the path in its wake by depositing an inactive material or by recruiting other agents to deposit the material or to self-assemble to become the path. In effect, the path forming process needs to be implemented by a more specific, physically realizable description.

We will use this process to illustrate our provisional morphogenetic programming notation, which is described in more detail elsewhere [21,23,24,26]. The central notion is a *substance*, which defines a kind of material by specifying its properties and the equations governing them.

We begin with a definition of the medium through which the attractant diffuses. The principal variable is A , attractant concentration, but there is also G , which represents the concentration of goal (or destination) markers, and P , which represents the concentration of markers for new or existing paths. Various parameters govern diffusion and degradation.

substance medium:

scalar fields:

A	attractant concentration
G	goal concentration
P	path concentration

order-2 field \mathbf{D}_A || attractant diffusion

scalars:

τ_A	attractant decay constant
γ	attractant deposition accel. rate
τ_P	path clamping constant

behavior:

|| diffusion – decay + goal signaling – path clamping:

$$\partial A = \mathbf{D}_A \nabla^2 A - A/\tau_A + \gamma G A - P/\tau_P.$$

The behavioral equation describes the change in attractant concentration. The first two terms are attractant diffusion and degradation (in which we use $\nabla^2 = \nabla \cdot \nabla$ for the Laplacian operator on tensor fields), the third term defines accelerating generation of attractant in the goal region and the fourth term represents the elimination of attractant in existing and new paths (assuming $\tau_P \ll \tau_A$). \mathbf{D}_A is

defined to be an *order-2 field*, which means that it is a 3×3 tensor defined at every point in space; it determines the diffusibility of the medium in each direction at every location.

The growth cone is a body composed of a substance that we call *neurite*, which is defined:

substance neurite:

scalar field C	neurite concentration
vector field \mathbf{v}	velocity field
order-2 field σ	neurite diffusion tensor
order-1 random \mathbf{W}	random motion

scalars:

α	cone migration rate
β	path deposition rate

behavior:

|| go approximately in gradient direction:

$$\mathbf{v} = \alpha(\nabla A / \|\nabla A\| + \sigma \mathbf{W})$$

$$\partial \mathbf{p} = \mathbf{v}$$

|| concentration change in material frame:

$$\partial C = -\nabla \cdot (C \mathbf{v}) + \mathbf{v} \cdot \nabla C$$

$$\partial P = \beta C \quad || \text{deposit path.}$$

The equation for \mathbf{v} causes neurites to move at a constant rate in the direction of the attractant gradient, but with a random perturbation $\sigma \mathbf{W}$ (to ensure paths do not get stuck). For simplicity, all points of a growth cone (neurite body) move with identical velocity (i.e., the stochastic element affects all points identically). The change equation for \mathbf{p} , the predefined position vector, causes the neurite body to deform in accord with the velocity field. The change equation for C describes the change in concentration (which constitutes the motion of the growth cone) in the material frame. Finally, the change equation for P describes the deposition of path substance in the wake of the growth cone.

Having defined the substances and their behaviors, it remains to specify the *bodies* (tissues) composed of those substances and their initial states. In this simple example, there are two bodies, the growth cone in its original location and the goal (destination) marker. The goal body is initialized:

body Goal of medium:

for $\|\mathbf{p} - \mathbf{g}\| \leq 0.001$:

$$A = 1$$

$$G = 1$$

for $\|\mathbf{p} - \mathbf{g}\| > 0.001$:

$$A = 0$$

$$G = 0.$$

For the sake of the example, we have defined Goal to be a body of attractant within a radius of 0.001 (arbitrary units) of \mathbf{g} , the location of the goal. Initialization of the parameters (\mathbf{g} , \mathbf{D}_A , τ_A , γ , τ_P) is omitted for clarity. We have also omitted initialization of P to allow for the possibility of already formed paths.

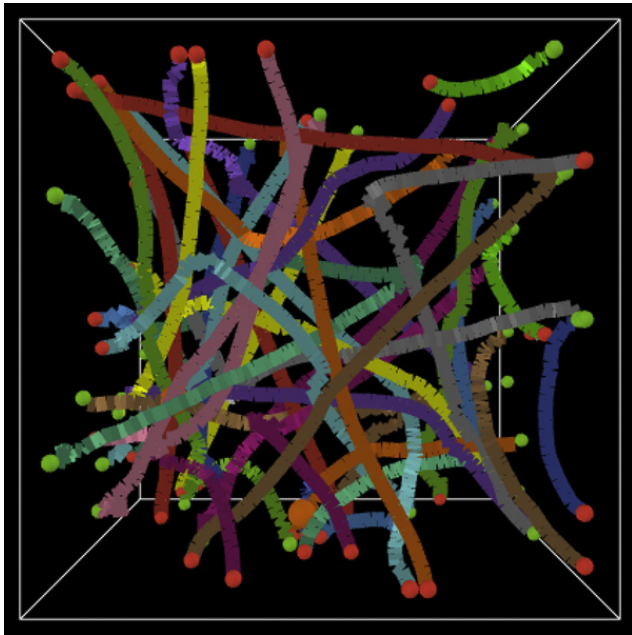


Fig. 3. Simulation of path growth process. In this example, 40 paths, occupying approximately 5% of the medium, were produced. In each case random origin and destination points were chosen on the four surrounding surfaces of a cube of the medium, and the algorithm was allowed to create a path.

The growth cone, which is a body of neurite substance, is initialized to a small region around \mathbf{s} , the source or origin of the path (definition omitted):

body GrowthCone of neurite:

$$\mathbf{v} = 0$$

$$\text{for } \|\mathbf{p} - \mathbf{s}\| \leq 0.001: C = 1$$

$$\text{for } \|\mathbf{p} - \mathbf{s}\| > 0.001: C = 0.$$

This morphogenetic program defines the routing of a path from a specified source \mathbf{s} to a specified destination \mathbf{g} , avoiding existing paths in the process. In the usual case many such paths would be needed. This can be accomplished by having different attractant substances and neurite substances attracted to them, or by creating the paths sequentially. We have simulated the latter process.

Fig. 3 shows the results of simulating a sequential multiple path routing process. In this example, 40 paths, occupying approximately 5% of the medium, were produced. In each case random origin and destination points were chosen on four surrounding surfaces of a cube of the medium, and the algorithm was allowed to create a path. After each path was complete, a time delay permitted the attractant to diffuse and degrade to background levels before picking the next origin and destination. This decreased the likelihood of one path interfering with the routing of the next, which still occurs in a few cases (where a path makes a sharp, unnecessary turn).

6. Example: assembling a segmented body with segmented legs

For another example, we will demonstrate how an artificial morphogenetic process might be developed to self-assemble a moderately complex hierarchical structure. Our

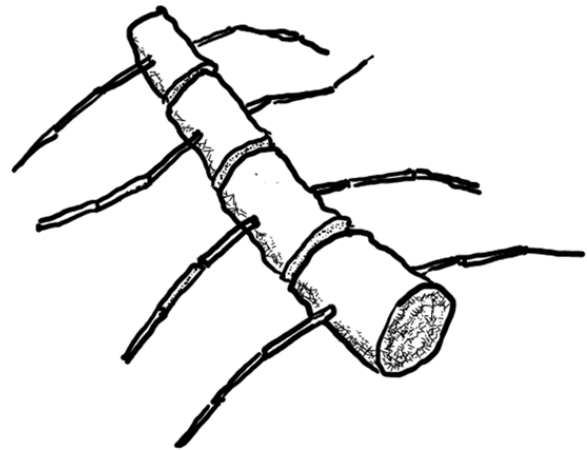


Fig. 4. Sketch of goal object for artificial morphogenesis. The number and length of the body and leg segments should be controllable.

goal is to assemble structures like that sketched in Fig. 4, with the additional requirement that we are able to control the number and length of the body segments and the number and length of the leg segments (assumed to be the same for all legs). The assembled structure is reminiscent of an insect body and might be the skeletal frame for a robot. However, we must stress that this is not an actual biological form, and so we are not duplicating any natural morphogenetic process. Rather, we are using the same basic processes that occur in nature, but deploying them in a different way to coordinate the assembly of an artificial structure.

The assembly takes place in two phases: assembling the body and assembling the legs. The first phase is inspired by the *clock-and-wavefront process* that governs the formation of spinal segments in vertebrates [10]. Since vertebra numbers are characteristic of a species, but vary from species to species, this process can be controlled as required. In the second phase, the same process is used to assemble segmented legs at the locations required. (Although the result is reminiscent of an insect body, this is not the morphogenetic process by which insect bodies or vertebrate limbs develop.)

6.1. Assembling the body

Differentiation of the spinal segments is a precursor to the formation of *somites*, which help to organize an embryo's body by governing the placement of internal organs and other structures. Many models of the segmentation process have been proposed [10,12,17,2–4], but experimental evidence now favors the clock-and-wavefront process. In this process, the growing embryo's tail bud contains a pacemaker, which periodically generates a signal that propagates toward the head region (see simulation in Fig. 5). Formation of a new segment is governed by two morphogens, one diffusing headward from the tail bud and the other diffusing tailward from the segments that have already formed. The new segment forms in a region of relatively low concentration of these two morphogens. The number of segments is determined by the ratio of the duration of spinal elongation to the clock period, and the length of the segments is controlled by the ratio of the growth rate

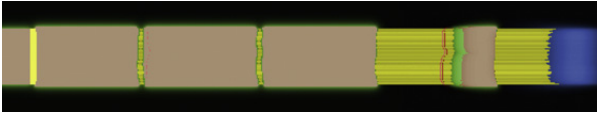


Fig. 5. Two-dimensional simulation of clock-and-wavefront segmentation process. “Head” to left, “tail” to right. The figure shows four completed segments and a fifth in the process of differentiation; the left-most, “head” segment was initialized and not a result of morphogenesis. The right-most (blue) area represents caudal (tail) morphogen diffusing from the rightward-moving tail bud (not visible). The green fuzziness around the segments represents a rostral (head) morphogen diffusing from partially or completely differentiated segments. The striated yellow color between segments represents undifferentiated tissue. The tail bud periodically generates a clock signal, which propagates toward the left as a wavefront, visible as a doubled red line in the undifferentiated tissue between the right-most differentiated segment and the partially differentiated segment. (The preceding wavefront is faintly visible as a dotted line near the left edge of the third segment.) New segments differentiate in a region between the completed segments and the tail bud where both the rostral and caudal morphogen concentrations are below thresholds, which keeps the segments distinct. (For interpretation of the references to colour in this figure legend, the reader is referred to the web version of this article.)

to the clock frequency. Next these intuitive ideas have to be expressed mathematically, as a morphogenetic program.

The duration of growth is determined by a quantity G governed by $\partial G = -G/\tau_G$. Growth continues so long as this quantity is above a threshold ϑ_G . Since $G_t = G_0 \exp(-t/\tau_G)$, the duration of growth is $t_G = \tau_G \ln(G_0/\vartheta_G)$.

The terminal (“tail-bud”) tissue moves in the caudal direction, leaving undifferentiated tissue in its wake (see Fig. 6). The equations do not specify whether this occurs through proliferation of cells by mitosis, as it occurs in embryos, or by recruiting new agents from outside the structure, as might be the case for robotic self-assembly. The terminal cells are initialized with a caudal orientation \mathbf{u} and they move at a rate r_0 so long as growth continues. This can be expressed by a conditional equation: $r = [G > \vartheta_G]r_0$, where r is the effective rate of movement. Therefore the elongation of the body is

$$\lambda_B = r_0 \tau_G \ln(G_0/\vartheta_G). \quad (1)$$

The change in density T of terminal tissue is given then by the negative divergence of the flux:

$$\partial T = -\nabla(rT\mathbf{u}) = -r(\mathbf{u} \cdot \nabla T + T\nabla \cdot \mathbf{u}).$$

Then the change of density of undifferentiated tissue M in the wake of the tail bud is $\partial M = rT/\lambda_{TB}$, where λ_{TB} is the length of the tail bud. As noted, this could be a consequence of reproduction or of the recruiting of new agents.



(a) Density T of tissue in terminal (tail-bud) state.



(b) Density M of undifferentiated body tissue.

Fig. 6. Simulation of growth process.

The clock-and-wavefront process depends on the fact that the tissue is an *active medium*. That is, if an area of the tissue is sufficiently stimulated, it will “fire” and stimulate adjacent regions. Thus the area of activation will spread. However, after a region fires, it enters a *refractory period* during which it cannot fire again. Thus, activation propagates in one direction as a wavefront, which is one half of the clock-and-wavefront process (see Fig. 7(d)).

The clock part is contributed by the terminal cells, which fire at regular intervals, causing a train of wavefronts to propagate through the tissue. In our case, the clock signal varies sinusoidally, $\partial^2 K = -\omega^2 K$, but any periodic process would work as well; the frequency is ω .

The ratio of the tail growth rate to the clock frequency (in cycles per unit time) gives the length of the segments; thus, the segment length is $2\pi r_0/\omega$. Similarly, the product of the clock frequency (in cycles per unit time) and the growth duration t_G gives the number of segments, i.e., $\lfloor \omega t_G/2\pi \rfloor$.

To define the behavior of the active medium, we use two quantities; α is the concentration of a morphogen, which represents the activity of the active medium, and ϱ is the concentration of the recovery variable, which governs the refractory period. For convenience, we define another quantity ϕ that represents the density of cells that will fire, that is, for which morphogen concentration α is above threshold and the recovery variable ϱ is below threshold. Since M represents the cell density, the density of cells that will fire is given by:

$$\phi = [\alpha > \vartheta_\alpha \wedge \varrho < \vartheta_\varrho]M. \quad (2)$$

Next we break the change of α into two components, the first of which is subject to the clock. So long as growth continues ($G > \vartheta_G$), terminal cells with their clock over threshold ($K > \vartheta_K$) contribute a pulse of morphogen:

$$\partial \alpha += [G > \vartheta_G \wedge K > \vartheta_K]T.$$

The morphogen diffuses at a rate D_α (which is how the activation spreads) and decays at a rate τ_α (so that the medium does not saturate). Furthermore, non-refractory tissue with a morphogen concentration above threshold will fire. Therefore the second partial equation for morphogen change is

$$\partial \alpha += \phi + D_\alpha \nabla^2 \alpha - \alpha/\tau_\alpha.$$

A tissue that fires also adds an impulse to its recovery variable, which blocks further firing until the refractory period is over, as determined by the recovery variable decaying below its threshold:

$$\partial \varrho = \phi - \varrho/\tau_\varrho.$$

Note that the sudden increase in ϱ resets ϕ to 0 (Eq. (2)).



(a) Density C of caudal (posterior) morphogen diffusing from tail cells.



(b) Density S of differentiated segmentation tissue.



(c) Density R of rostral (anterior) morphogen diffusing from differentiated segments. Note that it is blocked from the partially differentiated segment.



(d) Concentration α of segmentation signal propagating to left.

Fig. 7. Simulation of clock-and-wavefront segmentation process. Four segments (brown color) are complete on the left and a fifth segment is differentiating. (For interpretation of the references to colour in this figure legend, the reader is referred to the web version of this article.)

Differentiation of an undifferentiated tissue into a segment is governed by two morphogens, a *caudal morphogen* that diffuses from the caudal (tail) region and a *rostral morphogen* that diffuses from the rostral (head) region and from previously differentiated segments. These morphogens represent proximity to the tail and to segmented regions, respectively. Therefore the new segment differentiates in a region where both morphogens are below threshold (as is explained later); see Fig. 7.

The concentration C of caudal morphogen increases at a rate κ_C and saturates in the terminal region ($T > 0$), from which it diffuses and decays at specified rates (D_C, τ_C):

$$\partial C = \kappa_C T(1 - C) + D_C \nabla^2 C - C/\tau_C.$$

The concentration R of rostral morphogen similarly increases in differentiated segment tissue ($S > 0$), from which it diffuses and decays, but there are two complications. First, the head region is initialized in a fully differentiated state ($S = 1$). Second, as is explained below, the passage of the wavefront can lead to premature generation of the rostral morphogen, so it is necessary to block it for a time. For this we use a rostral morphogen block signal B (defined later, Eq. (4)) that blocks production of R until it is below its threshold ϑ_B . The saturation of rostral morphogens in unblocked differentiated segments is defined by this partial equation:

$$\partial R = [B < \vartheta_B] \kappa_R S(1 - R). \quad (3)$$

Diffusion and decay of the morphogen are defined as usual:

$$\partial R = D_R \nabla^2 R - R/\tau_R.$$

Segmentation (differentiation into segmented tissue) takes place when a sufficiently strong segmentation signal ($\alpha > \alpha_{lwb}$) passes through a region that is sufficient far from the tail ($C < C_{upb}$) and sufficiently far from previous

segments ($R < R_{upb}$); see Fig. 7(c). For convenience we define a segmentation variable,

$$\zeta = [\alpha > \alpha_{lwb} \wedge C < C_{upb} \wedge R < R_{upb}] c_\zeta,$$

which defines an impulse as the α wave passes. The following change equation defines the increase in the density of differentiated tissue S under these conditions; once this process begins, differentiation continues until it is complete ($S = 1$):

$$\partial S = \zeta + \kappa_S S(1 - S).$$

The passage of the wavefront through the future segment initializes the caudal morphogen block used in Eq. (3):

$$\partial B = \zeta + B/\tau_B. \quad (4)$$

For many purposes, in biological morphogenesis as well as in artificial morphogenesis, it is necessary to distinguish the posterior part of a segment from its anterior part. Therefore we define quantities P and A that represent, respectively, the density of differentiated posterior and anterior segment tissue (Fig. 8(a) and (b)). A segment tissue ($S > 1$) differentiates into posterior border tissue when the segmentation signal passes through ($\alpha > \alpha_{lwb}$), and the caudal morphogen concentration (C) is in a specified range, ($P_{lwb} C_{upb}, P_{upb} C_{upb}$):

$$\begin{aligned} \partial P &= [P_{upb} C_{upb} > C > P_{lwb} C_{upb} \wedge \alpha > \alpha_{lwb}] c_P, \\ \partial P &= \kappa_P S P(1 - P). \end{aligned}$$

Anterior border tissue differentiates under analogous conditions:

$$\begin{aligned} \partial A &= [A_{upb} R_{upb} > R > A_{lwb} R_{upb} \wedge \alpha > \alpha_{lwb}] c_A, \\ \partial A &= \kappa_A S A(1 - A). \end{aligned}$$

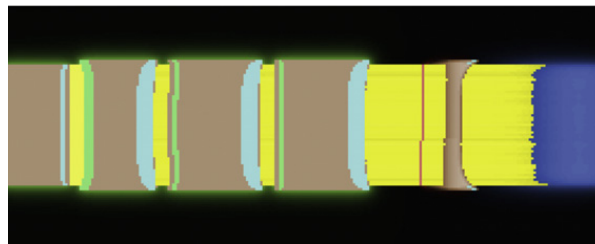
Fig. 8(c) is a composite representation of undifferentiated tissue, differentiated segments, and differentiated anterior and posterior regions; four segments are complete and a fifth is differentiating.



(a) Density of posterior segment tissue.



(b) Density of anterior segment tissue.



(c) Composite image showing dominant concentrations in each region.

Fig. 8. Differentiation of posterior and anterior segment borders.

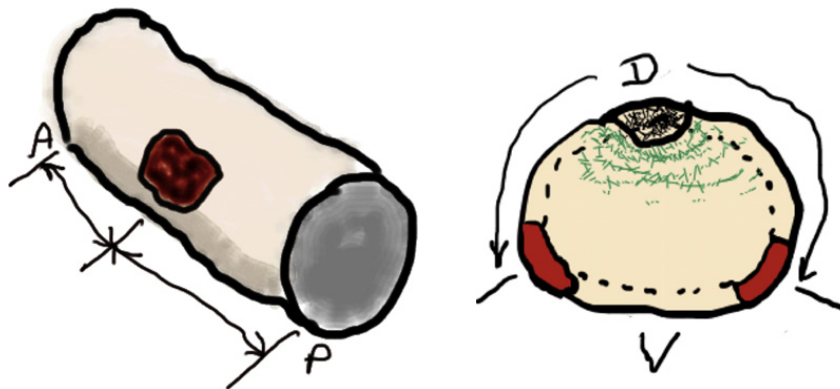


Fig. 9. Sketches indicating desired control over placement within segments of “imaginal disks” where appendages will be assembled.

6.2. Assembling the appendages

In the second phase of assembly, we use the same clock-and-wavefront process to assemble two segmented appendages on each body segment. These “legs” grow out of “imaginal disks” and so the position of the legs is controlled by the differentiation of segment tissue into imaginal disk tissue. As the sketches in Fig. 9 indicate, we want to control the anterior–posterior position of the imaginal disks within each segment, and their angular position relative to the dorsal–ventral axis.

Although the simulations illustrated in the preceding figures are two-dimensional, it is important to recognize that the morphogenetic equations of Section 6.1 apply as well in three dimensions as in two. That will not be the case in this section, in which for simplicity we limit the process to two dimensions. Therefore, while we control the anterior–posterior position of the imaginal disks, we will not address their angular position.

Control of anterior–posterior position is straightforward (Fig. 10). The anterior and posterior border tissues

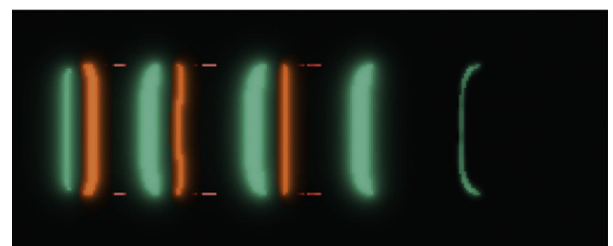


Fig. 10. Differentiation of imaginal disks on the surface of the body between anterior and posterior morphogens.

(A and P , respectively) emit anterior and posterior morphogens (a , p), which diffuse and degrade

$$\partial_t a = [A > \vartheta_A] \kappa_a S(1 - a) + D_a \nabla^2 a - a/\tau_a,$$

$$\partial_t p = [P > \vartheta_P] \kappa_p S(1 - p) + D_p \nabla^2 p - p/\tau_p.$$

The morphogens saturate in segment tissue ($S > 0$) where the anterior or posterior border cells are above their thresholds ($A > \vartheta_A$, $P > \vartheta_P$). These a and p morphogens establish opposing gradients by which anterior–posterior

position can be determined, namely where they are below specified thresholds (a_{upb} and p_{upb} ; see below).

However these conditions will obtain in a disk (in the three-dimensional case) or a band (in the two-dimensional case) transecting the body segment, whereas the imaginal disk tissue should be on the surface of the segment. Fortunately, it is relatively simple for cells to determine if they are at or near the surface of the body. *Quorum sensing* is a process by which bacteria and other microorganisms determine if their population density is sufficient for some purpose [11, pp. 192–4]. It can be implemented by secreting a degradable, diffusible substance and determining if it is above some threshold. In our case, we want to do “inverse quorum sensing,” since cells in the interior will be surrounded by cells on every side, whereas those near the surface will have neighbors on approximately half or less of their surfaces. Rather than explicitly modeling quorum sensing, we can convolve the differentiated-cell density S with a Gaussian kernel γ , which computes the average local density. Therefore cells near the edge will have a neighborhood density lower than some threshold, $\gamma \otimes S < S_{\text{upb}}$. We can now write the equation for the differentiation of the imaginal disks (I), which occurs in segment cells near the surface of the body where the anterior and posterior morphogens are in specified ranges (Fig. 10):

$$\begin{aligned} \text{DI} = [a_{\text{upb}} > a > a_{\text{lwb}} \wedge p_{\text{upb}} > p > p_{\text{lwb}} \\ \wedge \gamma \otimes S < S_{\text{upb}}]S(1 - I). \end{aligned}$$

Sufficiently rapid differentiation of the imaginal disks ($\text{DI} > \vartheta_{\text{DI}}$) triggers a number of changes in the tissue, which prepare the way for the growth and segmentation of the appendages, a process that uses the same clock-and-wavefront process as the body, and indeed shares many of the mechanisms. First, imaginal disk tissue differentiates into terminal (T) tissue, which behaves the same as it did in the tail bud, moving and leaving undifferentiated (M) tissue in its wake. However, there are several differences. First, the direction of motion is out from the body, rather than toward the tail. This is accomplished by setting the motion direction vector to point down the gradient of segmented tissue density, $\mathbf{u} = -\nabla S / \|\nabla S\|$, which can be implemented using the same signal used for quorum sensing.

Next, since the appendages have different lengths and segment numbers from the body, the parameters that control these must be different in appendage tissue and the terminal tissue that assembles it. The simplest way to control appendage length is by resetting the growth timer G to an appropriate value G_A . Therefore we use the same growth rate r_0 , decay rate τ_G , and threshold ϑ_G in the appendages as in the body. Solving Eq. (1) for G_0 gives the initial G value for appendages of length λ_A : $G_A = \vartheta_G \exp(\lambda_A / r_0 \tau_G)$.

The number and length of the segments in each appendage is most easily controlled by setting the clock frequency ω in the terminal cells that generate them; the clock variables (K, DK) are also reset to their initial values. For n segments, the correct frequency is $\omega_A = 2\pi nr_0 / \lambda_A$.

7. Conclusions

We have argued that reaping the full benefit of nanotechnology will require the ability to assemble complex systems that are hierarchically structured from the macroscale down to the nanoscale, but that this ability will require novel approaches to active self-assembly. The best model we have of these processes is embryological morphogenesis, and therefore we proposed artificial morphogenesis as an approach. We reviewed the fundamental processes in embryological development and argued that these processes, or approximations to them, will be feasible in artificial morphogenetic systems. Nevertheless, there are differences between natural and artificial systems, which future research must address. We explained the approach we are taking toward morphogenetic programming, and presented two examples, the routing of neuron-like connections and the assembly of a segmented body frame with segmented legs. We conclude that artificial morphogenesis shows promise as a means of coordinating the self-assembly of very large numbers of microscopic agents into complex hierarchical structures.

References

- [1] H. Abelson, D. Allen, D. Coore, C. Hanson, G. Homsy, T.F. Knight Jr., R. Nagpal, E. Rauch, G.J. Sussman, R. Weiss, Amorphous computing, *Communications of the ACM* 43 (5) (2000) 74–82.
- [2] R.E. Baker, S. Schnell, P.K. Maini, Formation of vertebral precursors: past models and future predictions, *Journal of Theoretical Medicine* 5 (1) (2003) 23–35.
- [3] R. Baker, S. Schnell, P. Maini, A mathematical investigation of a clock and wavefront model for somitogenesis, *Journal of Mathematical Biology* 52 (2006) 458–482, doi:10.1007/s00285-005-0362-2.
- [4] R. Baker, S. Schnell, P. Maini, A clock and wavefront mechanism for somite formation, *Developmental Biology* 293 (2006) 116–126.
- [5] D.A. Beysens, G. Forgacs, J.A. Glazier, Cell sorting is analogous to phase ordering in fluids, *Proceedings of the National Academy of Sciences of the United States of America* 97 (2000) 9467–9471.
- [6] E. Bonabeau, From classical models of morphogenesis to agent-based models of pattern formation, *Artificial Life* 3 (1997) 191–211.
- [7] D. Bray, Protein molecules as computational elements in living cells, *Nature* 376 (1995) 307–312.
- [8] D. Bray, *Wetware: A Computer in Every Living Cell*, Yale University Press, New Haven, 2009.
- [9] T.M. Cickovski, C. Huang, R. Chaturvedi, T. Glimm, H.G.E. Hentschel, M.S. Alber, J.A. Glazier, S.A. Newman, J.A. Izaguirre, A framework for three-dimensional simulation of morphogenesis, *IEEE/ACM Transactions on Computational Biology and Bioinformatics* 2 (4) (2005) 273–288.
- [10] J. Cooke, E.C. Zeeman, A clock and wavefront model for control of the number of repeated structures during animal morphogenesis, *Journal of Theoretical Biology* 58 (1976) 455–476.
- [11] J.A. Davies, *Mechanisms of Morphogenesis*, Elsevier, Amsterdam, 2005.
- [12] M.-L. Dequéant, O. Pourquié, Segmental patterning of the vertebrate embryonic axis, *Nature Reviews Genetics* 9 (2008) 370–382.
- [13] G.M. Edelman, *Topobiology: An Introduction to Molecular Embryology*, Basic Books, New York, 1988.
- [14] K.W. Fleischer, A multiple-mechanism developmental model for defining self-organizing geometric structures, Ph.D. Thesis, California Institute of Technology, Pasadena, CA, 1995.
- [15] G. Forgacs, S.A. Newman, *Biological Physics of the Developing Embryo*, Cambridge University Press, Cambridge, UK, 2005.
- [16] S.C. Goldstein, J.D. Campbell, T.C. Mowry, Programmable matter, *Computer* 38 (6) (2005) 99–101.
- [17] C. Gomez, E.M. Özbudak, J. Wunderlich, D. Baumann, J. Lewis, O. Pourquié, Control of segment number in vertebrate embryos, *Nature* 454 (2008) 335–339.

- [18] P. Hogeweg, Evolving mechanisms of morphogenesis: on the interplay between differential adhesion and cell differentiation, *Journal of Theoretical Biology* 203 (2000) 317–333, doi:10.1006/jtbi.2000.1087.
- [19] B.J. MacLennan, Embodiment and non-Turing computation, in: 2008 North American Computing and Philosophy Conference: The Limits of Computation, The International Association for Computing and Philosophy, Bloomington, IN, 2008. URL: <http://www.cs.utk.edu/~mclennan/papers/AEC-TR.pdf>.
- [20] B.J. MacLennan, Computation and nanotechnology (editorial preface), *International Journal of Nanotechnology and Molecular Computation* 1 (1) (2009) i–ix.
- [21] B.J. MacLennan, Preliminary development of a formalism for embodied computation and morphogenesis, Technical Report UT-CS-09-644, Department of Electrical Engineering and Computer Science, University of Tennessee, Knoxville, TN, 2009.
- [22] B.J. MacLennan, The U-machine: a model of generalized computation, *International Journal of Unconventional Computing* 6 (2010) 265–283.
- [23] B.J. MacLennan, Morphogenesis as a model for nano communication, *Nano Communication Networks* 1 (3) (2010) 199–208, doi:10.1016/j.nancom.2010.09.007.
- [24] B.J. MacLennan, Models and mechanisms for artificial morphogenesis, in: F. Peper, H. Umeo, N. Matsui, T. Isokawa (Eds.), *Proceedings in Information and Communications Technology, PICT*, in: *Natural Computing, Springer Series*, vol. 2, Springer, Tokyo, 2010, pp. 23–33.
- [25] B.J. MacLennan, Embodied computation: applying the physics of computation to artificial morphogenesis, in: M. Stannett (Ed.), *Proceedings of the Satellite Workshops of UC 2011 Unconventional Computation*, in: *TUCS Lecture Notes*, vol. 14, Turku Centre for Computer Science, University of Turku, Turku, Finland, 2011, pp. 9–20.
- [26] B.J. MacLennan, Artificial morphogenesis as an example of embodied computation, *International Journal of Unconventional Computing* 7 (1–2) (2011) 3–23.
- [27] H. Meinhardt, *Models of Biological Pattern Formation*, Academic Press, London, 1982.
- [28] S. Murata, H. Kurokawa, Self-reconfigurable robots: shape-changing cellular robots can exceed conventional robot flexibility, *IEEE Robotics & Automation Magazine* (2007) 71–78.
- [29] R. Nagpal, A. Kondacs, C. Chang, Programming methodology for biologically-inspired self-assembling systems, in: *AAAI Spring Symposium on Computational Synthesis: From Basic Building Blocks to High Level Functionality*, 2003, pp. 173–180. URL: <http://www.eecs.harvard.edu/ssr/papers/aaaiSS03-nagpal.pdf>.
- [30] I. Salazar-Ciudad, J. Jernvall, S. Newman, Mechanisms of pattern formation in development and evolution, *Development* 130 (2003) 2027–2037.
- [31] L.A. Taber, *Nonlinear Theory of Elasticity: Applications in Biomechanics*, World Scientific, Singapore, 2004.
- [32] C.J. Tomlin, J.D. Axelrod, Biology by numbers: mathematical modelling in developmental biology, *Nature Reviews Genetics* 8 (2007) 331–340.
- [33] A. Turing, The chemical basis of morphogenesis, *Philosophical Transactions of the Royal Society B* 237 (1952) 37–72.
- [34] A. van Wijngaarden, B.J. Mailloux, J.E.L. Peck, C.H.A. Koster, Report on the algorithmic language ALGOL 68, *Numerische Mathematik* 14 (1969) 79–218.



Bruce J. MacLennan has a BS in mathematics (1972, Florida State University) and an MS (1974) and Ph.D. (1975) in computer science (Purdue University). He joined Intel in 1975 to work on computer architectures and languages. In 1979, he joined the Computer Science faculty of the Naval Postgraduate School, where he was Assistant Professor (1979–83), Associate Professor (1983–7), and Acting Chair (1984–5). Since 1987 he has been in the Electrical Engineering and Computer Science department of the University of Tennessee, Knoxville. His research now focuses on natural computation and self-organization applied to nanotechnology and new computing technologies.